AD-A096 193 ARMY ARMAMENT RESEARCH AND DEVELOPMENT COMMAND WATER--ETC F/G 20/11
RESIDUAL STRESS REDISTRIBUTION CAUSED BY NOTCHES AND CRACKS IN --ETC(U)
JAN 81 S L PU, M A HUSSAIN

UNCLASSIFIED ARLCB-TR-81005 SBIE-AD-E440 109 NL

END
DATE FILMED
4-81
DTIC

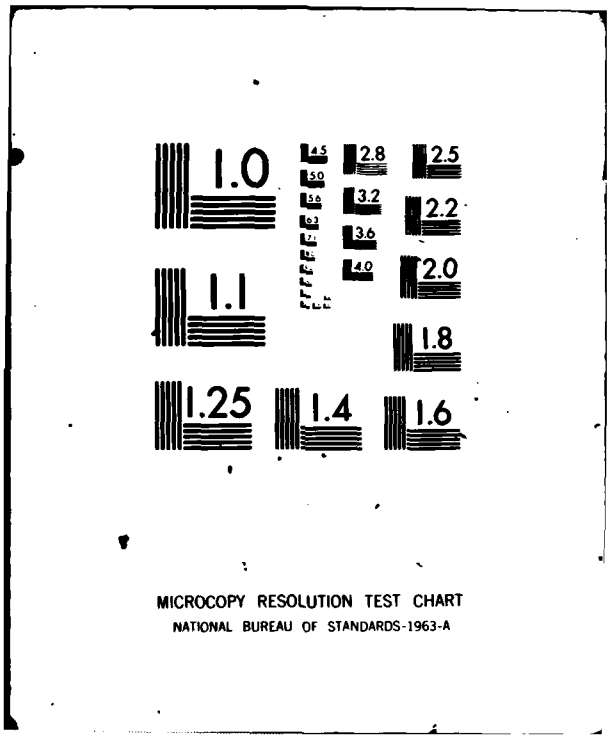
1.0
1.1
1.25
1.4
1.6
1.8
2.0
2.2
2.5
2.8
3.2
3.6
4.0
4.5
5.0
5.6
6.3
7.1
MICROCOPY RESOLUTION TEST CHART
NATIONAL BUREAU OF STANDARDS-1963-A

(12) LEVEL III

AD-E440109

AD

AD A096193

TECHNICAL REPORT ARLCB-TR-81005

RESIDUAL STRESS REDISTRIBUTION CAUSED BY NOTCHES AND CRACKS IN A PARTIALLY AUTOFRETTAGED TUBE

S. L. Pu
M. A. Hussain

January 1981

US ARMY ARMAMENT RESEARCH AND DEVELOPMENT COMMAND
LARGE CALIBER WEAPON SYSTEMS LABORATORY
BENÉT WEAPONS LABORATORY
WATERVLIET, N. Y. 12189

AMCMS No. 611102H600011

DA Project No. 1L161102AH60

PRON No. 1A0215601A1A

DTIC ELECTE S MAR 1 1 1981 D B

APPROVED FOR PUBLIC RELEASE; DISTRIBUTION UNLIMITED

DDC FILE COPY

81 2 23 043

DISCLAIMER

The findings in this report are not to be construed as an official Department of the Army position unless so designated by other authorized documents.

The use of trade name(s) and/or manufacturer(s) does not constitute an official indorsement or approval.

DISPOSITION

Destroy this report when it is no longer needed. Do not return it to the originator.

SECURITY CLASSIFICATION OF THIS PAGE (When Data Entered)

REPORT DOCUMENTATION PAGE	READ INSTRUCTIONS BEFORE COMPLETING FORM
1. REPORT NUMBER: ARLCB-TR-81005	2. GOVT ACCESSION NO.: AD-A096 193
3. RECIPIENT'S CATALOG NUMBER	
4. TITLE (and Subtitle): RESIDUAL STRESS REDISTRIBUTION CAUSED BY NOTCHES AND CRACKS IN A PARTIALLY AUTOFRETTAGED TUBE	5. TYPE OF REPORT & PERIOD COVERED
	6. PERFORMING ORG. REPORT NUMBER
7. AUTHOR(s): S. L. Pu and M. A. Hussain	8. CONTRACT OR GRANT NUMBER(s)
9. PERFORMING ORGANIZATION NAME AND ADDRESS: Benet Weapons Laboratory Watervliet Arsenal, Watervliet, NY 12189 DRDAR-LCB-TL	10. PROGRAM ELEMENT, PROJECT, TASK AREA & WORK UNIT NUMBERS: AMCMS No. 611102H600011 DA Project No. 1L161102AH60 PRON No. 1A0215601A1A
11. CONTROLLING OFFICE NAME AND ADDRESS: U.S. Army Armament Research & Development Command Large Caliber Weapon Systems Laboratory Dover, NJ 07801	12. REPORT DATE: January 1981 13. NUMBER OF PAGES: 21
14. MONITORING AGENCY NAME & ADDRESS(if different from Controlling Office)	15. SECURITY CLASS. (of this report): UNCLASSIFIED 15a. DECLASSIFICATION/DOWNGRADING SCHEDULE

16. DISTRIBUTION STATEMENT (of this Report)

Approved for public release; distribution unlimited.

17. DISTRIBUTION STATEMENT (of the abstract entered in Block 20, if different from Report)

18. SUPPLEMENTARY NOTES

To be published in Journal of Pressure Vessel Technology.

19. KEY WORDS (Continue on reverse side if necessary and identify by block number)

Stress Intensity
Residual Stress
Stress Redistribution
Autofrettaged Tube
Fracture Mechanics

20. ABSTRACT (Continue on reverse side if necessary and identify by block number)

A simple method is provided for the computation of the redistribution of residual stresses and the stress intensity factors due to the introduction of notches and cracks in a partially autofrettaged tube. Numerical results of several crack and notch problems are obtained by the method of thermal simulation. These results are shown to be in excellent agreement with those obtained from the classical method of superposition. The new method based on thermal simulation
(CONT'D ON REVERSE)

DD FORM 1 JAN 73 1473 EDITION OF 1 NOV 65 IS OBSOLETE UNCLASSIFIED

SECURITY CLASSIFICATION OF THIS PAGE (When Data Entered)

20. Abstract (Cont'd)

is easier to apply and it avoids the singular stresses near the crack tip when th distributed crack face loading is used in the method of superposition.

TABLE OF CONTENTS

	Page
NOMENCLATURE	ii
INTRODUCTION	1
THERMAL STRESS SIMULATION	2
STRESS INTENSITY FACTOR DUE TO THE RESIDUAL STRESS	5
STRESS REDISTRIBUTION	9
CRACKS INITIATED FROM NOTCHES	11
CONCLUSION	13
REFERENCES	14

TABLES

I. REDISTRIBUTION OF σ_θ DUE TO TWO ID NOTCHES IN A CYLINDER WITH 60% OVERSTRAIN.	10
II. REDISTRIBUTION OF σ_θ DUE TO TWO ID NOTCHES IN A CYLINDER WITH 100% OVERSTRAIN.	11

LIST OF ILLUSTRATIONS

1(a). Two equal and symmetric radial cracks in a tube.	15
1(b). Finite element idealization for Figure 1(a).	15
2(a). Residual stress normal to the cross section cc of a 100% overstrained tube.	16
2(b) and (c). Normal transactions on the crack surface.	16
3. Stress intensity factor due to the residual stress by superposition.	17
4(a). Two equal and symmetric notches in a tube.	18
4(b). Finite element idealization for Figure 4(a).	18
5. Two equal and symmetric radial cracks initiated from notches in a tube shown previously.	19

NOMENCLATURE

a	=	inner radius, 1" (2.54 cm)
b	=	outer radius, 2" (5.08 cm)
c-c	=	a radial cut passing through a radial crack
d	=	the depth of a radial crack, 0.2" (.508 cm)
r,θ	=	cylindrical coordinates
ρ	=	the radius of elastic-plastic interface during pressurization
σ	=	normal stress
σ_o	=	yield stress, 170 Ksi (1173 MPa)
T	=	temperature at r
T_a, T_ρ	=	temperature at r = a and r = ρ respectively
E	=	Young's modulus, 30 x 10^6 psi (207 GPa)
α	=	coefficient of thermal expansion, 6.8 x 10^{-6} in/in/°F (12.24 x 10^{-6} m/m/°C)
ν	=	Poisson's ratio, 0.3
K_I	=	mode I stress intensity factor, Ksi$\sqrt{in}$ = 1.1 MPa$\sqrt{m}$)

Accession For	
NTIS GRA&I	☑
DTIC TAB	☐
Unannounced	☐
Justification	
By	
Distribution/	
Availability Codes	
Dist	Avail and/or Special
A	

INTRODUCTION

A hollow cylinder is a common configuration used in pressure vessels. According to the classical Lame' solution for an elastic cylinder, the largest tangential stress occurs at the bore. In order to increase the maximum pressure a cylinder can contain, to reduce the probability rate of crack initiation at the bore and to slow down the growth rate of a fatigue crack, a residual compressive stress can be introduced near the internal boundary. "Autofrettage" is such a process used to produce the favorable residual stresses in a gun barrel. By swaging an oversized mandrel through the bore or by applying a sufficiently high hydrostatic pressure at the bore, the cylinder is partially yielded. Upon removal of the inner pressure, a residual stress distribution will result in the cylinder. The tangential stress is highly compressive at the bore and varies logarithmically to tension over the region which was plastically deformed during pressurization. The plane-strain residual stresses due to autofrettage are well-known. The residual stress pattern will change due to changes of geometrical configurations such as the presence of keyways, notches, cracks, etc. The redistribution of residual stresses in these instances is not generally straight forward.

In a previous article[1] we showed that an active thermal load can be used to produce thermal stresses equivalent to autofrettage residual stresses. This approach provides a method to find the redistribution of residual

---

[1]Hussain, M. A., Pu, S. L., Vasilakis, J. D., and O'Hara, P., "Simulation of Partial Autofrettage by Thermal Loads," Journal of Pressure Vessel Technology, Vol. 102, No. 3, 1980, pp. 314-318.

stresses by computing the thermal stresses in the cylinder with notches and cracks under the thermal load. In this report we supply numerical verification to show the equivalence of thermal and residual stress redistribution caused by notches and the equivalence in stress intensity factors for cracks due to residual stresses and simulated thermal loads. The method of superposition requires distributed loads on the crack face. It results in singular stresses near the crack tip from the finite element computations using APES. On the other hand, the method of thermal simulation is simple in application and yields accurate results including stresses near the crack tip.

THERMAL STRESS SIMULATION

The plane-strain stress distribution of a partially autofrettaged tube using the von Mises' yield condition and the incompressibility condition is given by[2]

$$\sigma_r = \begin{cases} \frac{\sigma_o}{\sqrt{3}} \left\{ (2 \log \frac{r}{\rho} - 1 + \frac{\rho^2}{b^2}) - P_1 (\frac{1}{b^2} - \frac{1}{r^2}) \right\} & a \leq r \leq \rho \quad (1) \\ \frac{\sigma_o}{\sqrt{3}} (\rho^2 - P_1)(\frac{1}{b^2} - \frac{1}{r^2}) & \rho \leq r \leq b \quad (2) \end{cases}$$

$$\sigma_\theta = \begin{cases} \frac{\sigma_o}{\sqrt{3}} \left\{ 2 \log \frac{r}{\rho} + 1 + \frac{\rho^2}{b^2} - P_1 (\frac{1}{b^2} + \frac{1}{r^2}) \right\} & a \leq r \leq \rho \quad (3) \\ \frac{\sigma_o}{\sqrt{3}} (\rho^2 - P_1)(\frac{1}{b^2} + \frac{1}{r^2}) & \rho \leq r \leq b \quad (4) \end{cases}$$

---

[2]Hill, R., The Mathematical Theory of Plasticity, Oxford at the Clarendon Press, 1950.

Where P_1, a constant depending on geometrical dimensions only,

$$P_1 = \frac{a^2b^2}{b^2-a^2}\left(1 - \frac{\rho^2}{b^2} + 2\log\frac{\rho}{a}\right) \tag{5}$$

Upon the application of the following thermal load

$$\begin{cases} T = T_a - \dfrac{(T_a-T_\rho)}{\log(\rho/a)}\log(r/a) & a \leq r \leq \rho \quad (6) \\ T = T_\rho & \rho \leq r \leq b \quad (7) \end{cases}$$

the thermal stresses in the hollow cylinder are[1]

$$\sigma_r = \begin{cases} \dfrac{E\alpha(T_a-T_\rho)}{2(1-\nu)\log(\rho/a)}\left\{\left(2\log\frac{r}{\rho} - 1 + \frac{\rho^2}{b^2}\right) - P_1\left(\frac{1}{b^2} - \frac{1}{r^2}\right)\right\} & a \leq r \leq \rho \\ \dfrac{E\alpha(T_a-T_\rho)}{2(1-\nu)\log(\rho/a)}\left(\rho^2-P_1\right)\left(\frac{1}{b^2} - \frac{1}{r^2}\right) & \rho \leq r \leq b \end{cases}$$

$$\sigma_\theta = \begin{cases} \dfrac{E\alpha(T_a-T_\rho)}{2(1-\nu)\log(\rho/a)}\left\{2\log\frac{r}{\rho} + 1 + \frac{\rho^2}{b^2} - P_1\left(\frac{1}{b^2} + \frac{1}{r^2}\right)\right\} & a \leq r \leq \rho \\ \dfrac{E\alpha(T_a-T_\rho)}{2(1-\nu)\log(\rho/a)}\left(\rho^2-P_1\right)\left(\frac{1}{b^2} + \frac{1}{r^2}\right) & \rho \leq r \leq b \end{cases}$$

---

[1]Hussain, M. A., Pu. S. L., Vasilakis, J. D., and O'Hara, P., "Simulation of Partial Autofrettage by Thermal Loads," Journal of Pressure Vessel Technology, Vol. 102, No. 3, 1980, pp. 314-318.

If the temperature gradient of the thermal load and the yield stress of the cylinder material satisfy the relation

$$\frac{E\alpha(Ta-T\rho)}{2(1-\nu)\log(\rho/a)} = \frac{2\sigma_o}{\sqrt{3}} \tag{8}$$

the thermal stresses and the autofrettage residual stresses become equivalent.

Using the temperature distributions as temperature input in a finite-difference computer program based on the theory of thermal stress in Sections 9-10 of reference 3, numerical results were obtained for the thermal stresses in a cylinder. These values were shown in reference 1 to be in good agreement with residual stresses computed from equations (1) to (4). Thermal stresses were also computed using the finite element NASTRAN program. The finite element results for the thermal stresses were also in excellent agreement with the autofrettage residual stresses.[1] It remains to be shown that the redistribution of thermal stresses due to the presence of geometrical discontinuities simulates the redistribution of residual stresses caused by the same geometrical changes. This question of simulation was specifically raised by a review of the work of Kapp,[4] who applied the idea of thermal load simulation to stress analysis of autofrettaged cylinders with an OD notch.

---

[1]Hussain, M. A., Pu, S. L., Vasilakis, J. D., and O'Hara, P., "Simulation of Partial Autofrettage by Thermal Loads," Journal of Pressure Vessel Technology, Vol. 102, No. 3, 1980, pp. 314-318.

[3]Boley, B. A. and Weiner, J. H., Theory of Thermal Stresses, John Wiley and Sons, 1960.

[4]Kapp, J. A. and Pflegl, G. A., "Stress Analysis of OD Notched Thick-Walled Cylinders Subjected to Internal Pressure or Thermal Loads," Technical Report ARLCB-TR-80005, Benet Weapons Laboratory, LCWSL, ARRADCOM, US Army, February 1980.

STRESS INTENSITY FACTOR DUE TO THE RESIDUAL STRESS

Consider a crack in the radial direction emanating from the outer boundary of an autofrettaged tube. The crack will be opened up due to the tensile residual stress in the circumferential direction. This will change the residual stress distribution in the tube. A method is required to compute the stress intensity factor due to the residual stress. The method of thermal simulation was proposed and used in reference 1. The method of superposition, which will be discussed below, is another. The result from the method of superposition is within one percent of that reported in reference 1 by the method of thermal simulation.

For an ID (inner diameter) radial crack, the crack remains closed in the compressive residual stress region. The stress intensity factor is zero and the crack does not affect the residual stress field. The crack will open when a sufficiently large internal pressure is applied on the inner boundary of the cylinder. The stress intensity factor is the net sum of two values, one is positive corresponding to the tensile stress due to the applied internal pressure and the other is negative due to the compressive residual stress. If the absolute value of the latter is larger than the former, the net result of the stress intensity factor is zero since negative stress intensity factor has no physical meaning. However for computational purposes, a negative stress intensity factor due to the compressive residual stress is convenient and should be understood as such. It is necessary to have an effective method for

---

[1]Hussain, M. A., Pu, S. L., Vasilakis, J. D., and O'Hara, P., "Simulation of Partial Autofrettage by Thermal Loads," Journal of Pressure Vessel Technology, Vol. 102, No. 3, 1980, pp. 314-318.

the computation of the stress intensity factor due to the compressive residual stress.

The thermal stress simulation mentioned in the previous section provides a method of computation of stress intensity factors due to residual stresses. The residual stress is replaced by an active thermal load which produces a thermal stress distribution identical to the residual stress. The stress intensity factor sought is obtained from that due to the thermal load.

The finite element computer program APES, using 12-node isoparametric elements, is used in all the numerical computations reported here. This powerful program has been continually expanded to add new features such as graphical output, thermal loading, crack face loading for enriched elements, etc., and to increase the capacity to handle a maximum of 200 elements.[5] The new thermal input feature of APES came just in time for the fracture analysis due to thermal loading.

As a first example, consider a cylinder with two ID cracks, Figure 1(a). From the symmetry of the problem, only the first quadrant of the cylinder is needed to be considered. The finite element idealization using two enriched elements at the crack tip is shown in Figure 1(b). The temperature at the bore is arbitrarily chosen to be $T_a = 0$. The temperature at the outer boundary can be computed from equation (8). It depends on the material constants

---

[5]Gifford, L. Nash, "APES-Finite Element Fracture Mechanics Analysis Revised Documentation," Naval Ship Research and Development Center Technical Report DTNSRDC-79/023, March 1979.

of the cylinder as well as the degree of overstrain. For a cylinder with E = 30 x 10^6 psi (207 GPa), ν = 0.3, α = 6.8 x 10^{-6} in/in/°F (12.24 x 10^{-6} cm/cm/°C), σ_o = 170 Ksi (1173 MPa), the temperature at the outside boundary is T_p = -633.17°F (-333.98°C) for 60% autofrettage. The same quantity for 100% autofrettage is T_p = -933.77°F (-500.98°C). For a crack depth d = 0.2 in. in a tube of b = 2 in., a = 1 in. the numerical results for the stress intensity factor due to the thermal load are K_1 = -89.403 Ksi$\sqrt{in}$ (1 Ksi $\sqrt{in}$ = 1.1 MPa$\sqrt{m}$) and K_1 = -109.63 Ksi$\sqrt{in}$ for 60% and 100% overstrained tubes, respectively. Using the well-known form of $K_1 = 1.12(\pi d)^{1/2}\sigma_o(r=a)$ for shallow edge cracks as a normalizing factor, the corresponding dimensionless stress intensity factors are $K_1/[1.12(\pi d)^{1/2}(\sigma_o)_a]$ = 0.70 and 0.74, respectively.

Another method based on the principle of superposition can be used to compute the stress intensity factor due to the autofrettage residual stress denoted by S_R. The tangential residual stress of S_R on the cross section c-c, Figure 1(a), for a 100% autofrettaged cylinder is shown in Figure 2(a). The stresses at r = a, a+d, and b are denoted by $(\sigma_\theta)_a$, $(\sigma_\theta)_d$ and $(\sigma_\theta)_b$, respectively. Let S_c be the normal traction distributed on the crack surface which tends to close the crack. Its magnitude is identical to the corresponding tangential residual stress of S_R as shown in Figure 2(b). The normal traction which is equal and opposite to S_c is designated by S_T, Figure 2(c). If both S_c and S_T are added to S_R, they produce no net effect, Figure 3(a). Now if S_T and S_R are combined, the crack surface is free of stress and remains closed. The stress intensity factor is of course zero, Figure 3(b). The negative stress intensity factor due to the normal traction S_c, Figure 3(c), must

equal the stress intensity factor due to S_R. The same finite element idealization of Figure 1(b) is used in the computer program to obtain the stress intensity factor due to S_c, which replaces the thermal load in the previous computation. The new feature of the APES program of crack face loading for enriched elements is used. The numerical result for a distributed load S_c corresponding to the 100% overstrain is $K_1 = -109.44$ Ksi$\sqrt{\text{in}}$. The percentage of error for the previous result due to thermal loading is 0.17%. This confirms that the thermal simulation gives a method for the computation of the stress intensity factor due to residual stress.

The APES program with the distributed crack face loading gives the correct stress intensity factor and singular stresses at the crack tip and its adjacent nodes. For instance, the stress σ_θ at the node nearest to and in front of the crack tip along the x-axis is -0.786×10^{49} psi. The thermal stress at the same node due to the simulated thermal load is $\sigma_\theta = -0.564 \times 10^6$ psi. From the stress intensity factor obtained, the normal stress can be estimated by the near field solution due to Westergaard[6]

$$\sigma_x = \frac{K_1}{\sqrt{\pi r}} \cos\frac{\theta}{2}\left[1 - \sin\frac{\theta}{2}\sin\frac{3\theta}{2}\right] \tag{9}$$

$$\sigma_y = \frac{K_1}{\sqrt{\pi r}} \cos\frac{\theta}{2}\left[1 + \sin\frac{\theta}{2}\sin\frac{3\theta}{2}\right] \tag{10}$$

---

[6]Westergaard, H. M., "Bearing Pressures and Cracks," Transactions of the ASME, Journal of Applied Mechanics, 1939.

For $\theta = 0$, $r = 0.015$ and $K_1 = -109.44$ Ksi$\sqrt{\text{in}}$, we have $\sigma_\theta = \sigma_y = -0.504 \times 10^6$ psi. The method of thermal simulation gives not only correct stress intensity factors for cracks, but also correct stresses even close to the crack tip.

STRESS REDISTRIBUTION

Due to the presence of notches, such as the two notches shown in Figure 4(a), redistribution of residual stresses occurs in the cylinder. To find the resultant residual stresses, thermal stress simulation may be used. The redistribution of thermal stresses due to the presence of notches under the simulated thermal load should be the same as residual stress redistribution. This will be verified numerically in what follows.

The redistribution of thermal stresses can be obtained numerically by the computer program APES. The finite element mesh of a quarter of the ring with one half of the notch is shown in Figure 4(b). The tangential thermal stresses at nodal points 1-10 along the x-axis and at nodal points 88-100 along the y-axis are tabulated in column (1) of Table I for a temperature gradient corresponding to 60% overstrain.

The redistribution of residual stresses can be computed based on the principle of superposition. Let S_R and S_R' be the residual stresses in the ring before and after the introduction of the notches. The compressive tangential stress on mn and the compressive radial stress on nq can be computed from equations (3) and (1) for the ring without the notch. The state of stress produced in the ring due to the distributed compressive stresses just obtained on mn and nq is denoted by S_C. Let S_T be equal and opposite to S_C. The redistribution of residual stresses, S_R', is not affected by adding S_C and S_T simultaneously.

The sum of S_R' and S_c is nothing but S_R. Hence S_R' is the sum of S_R and S_T. Exact values of tangential residual stress for S_R at the selected nodal points are tabulated in column (2) of Table I. The state of stress S_T can be computed by APES using the same finite element mesh, Figure 4(b), with the applied load distributed on mn and nq. The numerical results of σ_θ for S_T are given in column (3) of Table I. The sum of two values in columns (2) and (3) is σ_θ for S_R' given in column (4). The agreement between σ_θ in column (4) for S_R' and that in column (1) for thermal load is excellent.

Table II gives the similar comparison for the case of 100% overstrain.

TABLE I. REDISTRIBUTION OF σ_θ DUE TO TWO ID NOTCHES IN A CYLINDER WITH 60% OVERSTRAIN

		σ_θ in Ksi Corresponding to (1 Ksi = 6.9 MPa)			
Node (Fig. 4)	r/a	Thermal Load (1)	S_R (2)	S_T (3)	$S_R + S_T$ (4)
1	1.250	-210.20	- 38.91	-171.28	-210.19
2	1.3067	-146.75	- 20.96	-125.79	-146.75
3	1.3633	- 95.87	- 4.52	- 91.41	- 95.93
4	1.420	- 52.20	10.63	- 62.84	- 52.20
5	1.480	- 14.37	25.46	- 39.80	- 14.34
6	1.540	13.16	39.20	- 26.05	13.15
7	1.600	34.10	51.98	- 17.84	34.14
8	1.7333	45.85	47.29	- 1.46	45.83
9	1.8667	60.78	43.57	17.23	60.80
10	2.0	77.27	40.57	36.64	77.21
88	1.0	-116.63	-143.95	26.92	-117.03
89	1.0833	- 82.39	-103.08	20.98	- 82.10
90	1.1667	- 53.89	- 68.56	15.03	- 53.53
91	1.250	- 29.76	- 38.91	9.12	- 29.79
92	1.3067	- 14.11	- 20.96	6.55	- 14.41
93	1.3633	- 0.80	- 4.52	3.78	- 0.74
94	1.42	11.69	10.63	1.04	11.67
95	1.48	24.24	25.46	- 1.45	24.01
96	1.54	35.41	39.20	- 3.85	35.35
97	1.60	46.01	51.98	- 5.97	46.01
98	1.7333	36.95	47.24	- 10.48	36.81
99	1.8667	29.32	43.57	- 14.32	29.25
100	2.0	23.21	40.57	- 17.46	23.11

TABLE II. REDISTRIBUTION OF σ_θ DUE TO TWO ID NOTCHES IN A CYLINDER WITH 100% OVERSTRAIN

		σ_θ in Ksi Corresponding to (1 Ksi = 6.9 MPa)			
Node (Fig. 4)	r/a	Thermal Load (1)	S_R (2)	S_T (3)	$S_R + S_T$ (4)
1	1.250	-270.79	- 57.43	-213.39	-270.82
2	1.3067	-163.97	- 30.70	-133.26	-163.96
3	1.3633	- 85.48	- 7.14	- 78.41	- 85.55
4	1.420	- 31.11	13.84	- 44.89	- 31.05
5	1.480	9.74	32.72	- 22.74	9.78
6	1.540	41.27	49.85	- 8.62	41.23
7	1.600	65.80	65.49	0.31	65.80
8	1.7333	92.89	79.89	13.02	92.91
9	1.8667	122.06	93.21	28.85	122.05
10	2.0	151.66	105.59	46.06	151.65
88	1.0	-133.33	-166.54	32.68	-133.86
89	1.0833	- 98.89	-123.99	25.42	- 98.57
90	1.1667	- 70.45	- 88.15	18.16	- 69.99
91	1.250	- 46.36	- 57.43	11.09	- 46.34
92	1.3067	- 24.06	- 30.70	6.39	- 24.31
93	1.3633	- 5.69	- 7.14	1.58	- 5.56
94	1.420	11.03	13.84	- 2.86	10.98
95	1.480	28.38	32.72	- 6.60	26.12
96	1.540	39.69	49.85	- 10.14	39.71
97	1.600	52.41	65.49	- 13.22	52.27
98	1.7333	64.00	79.89	- 16.21	63.68
99	1.8667	74.47	93.21	- 18.87	74.34
100	2.0	84.30	105.59	- 21.25	84.34

CRACKS INITIATED FROM NOTCHES

In the previous example of two notches in an autofrettaged tube, two radial cracks are initiated from the notches, Figure 5. The stress intensity factor at the crack tip can be computed by the method of thermal simulation without additional complications. The same finite element idealization shown in Figure 4(b) is used here. However, elements (1) and (2) are enriched crack tip elements. The stress intensity factor for this problem is K_I = -100.87 Ksi$\sqrt{\text{in}}$ for a thermal load corresponding to 60% overstrain.

To use the method of superposition, it is logical to obtain the stress distribution along the crack line (nodes 1 to 4 in Figure 4) in the notched autofrettaged cylinder before the crack is actually introduced. This computation has been accomplished in the previous section. The results for a 60% overstrained cylinder are shown in Table I. Along the edge of element 1, where the radial crack will appear, the tangential stress components σ_θ are -210.19 Ksi, -146.75 Ksi, -95.93 Ksi and -52.20 Ksi at nodes 1, 2, 3, and 4, respectively. Applying this distributed crack face load as the only loading condition to the finite element idealization shown in Figure 4(b) again, with elements (1) and (2) being enriched crack tip elements, the APES program gives the stress intensity factor $K_I = -103.41$ Ksi$\sqrt{\text{in}}$. The percentage of error between this result and that obtained from thermal loading is about three percent. The higher percentage of error is due to the accumulation of errors in the repeated finite element computations in the method of superposition.

In the last example, the cracks appeared after the presence of the notches. The order of presence was maintained in the previous computation. However, the order is indifferent based on the principle of superposition in the linear theory of elasticity. If both the notches and the cracks are assumed to be present at the same time, it provides an alternative way for the computation of the stress intensity factor. Using the same finite element mesh shown in Figure 4(b), the stress intensity factor is computed for distributed loads applied on mn, nq, and the edge from node 1 to node 4 of element (1). The loads equal the normal stresses on mn, nq and on the edge of element (1) which we obtained from equations (3) and (1) for the autofrettaged cylinder without geometrical discontinuities. The stress intensity factor thus

obtained from APES is $K_1 = -100.81$ Ksi$\sqrt{in}$. It is in excellent agreement with $K_1 = -100.87$ Ksi$\sqrt{in}$ for the simulated thermal load.

With the method of superposition, it is necessary to apply the distributed load on the crack face which causes singular stress at and near the crack tip using the APES program. The thermal simulation method on the other hand gives quite accurate stress near the crack tip. For the combination of cracks and notches, the tangential thermal stress at node 5, Figure 4(b), is $\sigma_\theta = -215$ Ksi. The hoop stress estimated from the stress intensity factor based on equation (10) at the same node is $\sigma_\theta = -232$ Ksi.

CONCLUSION

The thermal stress simulation of residual stresses can be used for the computation of stress intensity factors for cracks and of stress redistribution due to the presence of cracks and notches in a residual stress field. Numerical results have shown the excellent agreement between thermal stress and residual stress and between the redistributions of thermal and residual stresses caused by notches and cracks. The method is simple and accurate and has some advantages over the classical method of superposition which results in singular stresses near the crack tip in the finite element computation.

REFERENCES

1. Hussain, M. A., Pu, S. L., Vasilakis, J. D., and O'Hara, P., "Simulation of Partial Autofrettage by Thermal Loads," Journal of Pressure Vessel Technology, Vol. 102, No. 3, 1980, pp. 314-318.
2. Hill, R., The Mathematical Theory of Plasticity, Oxford at the Clarendon Press, 1950.
3. Boley, B. A. and Weiner, J. H., Theory of Thermal Stresses, John Wiley and Sons, 1960.
4. Kapp, J. A., and Pflegl, G. A., "Stress Analysis of OD Notched Thick-Walled Cylinders Subjected to Internal Pressure or Thermal Loads," Technical Report ARLCB-TR-80005, Benet Weapons Laboratory, LCWSL, ARRADCOM, US Army, February 1980.
5. Gifford, L. Nash, "APES-Finite Element Fracture Mechanics Analysis Revised Documentation," Naval Ship Research and Development Center Technical Report DTNSRDC-79/023, March 1979.
6. Westergaard, H. M., "Bearing Pressures and Cracks," Transactions of the ASME, Journal of Applied Mechanics, 1939.

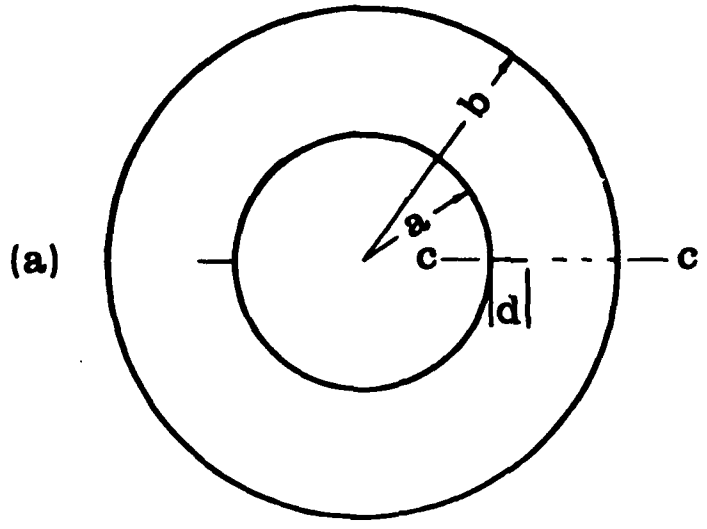

Figure 1(a). Two equal and symmetric radial cracks in a tube.

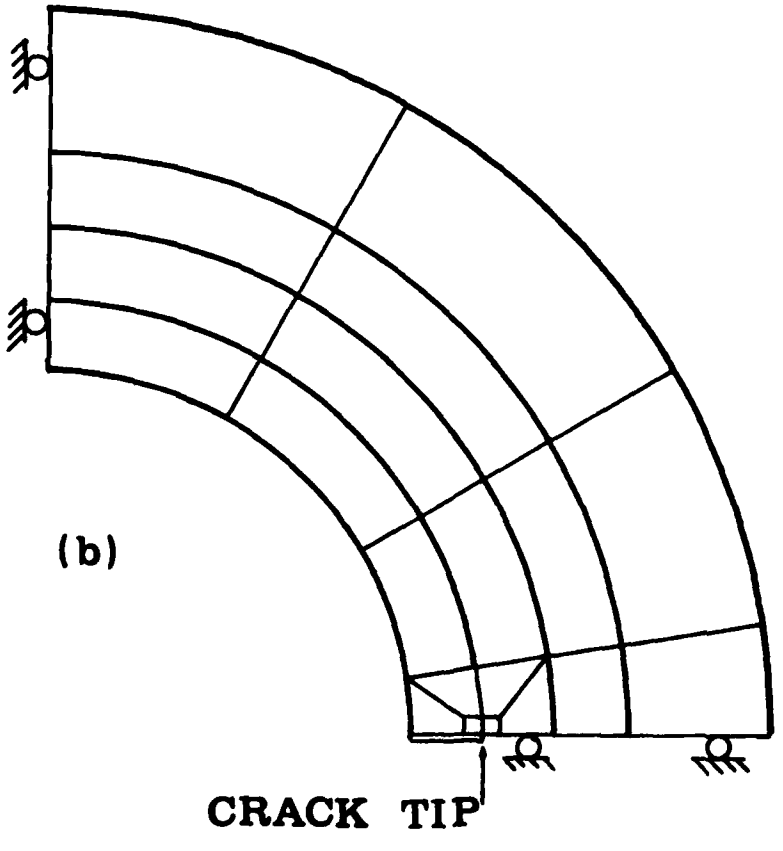

Figure 1(b). Finite element idealization for Figure 1(a).

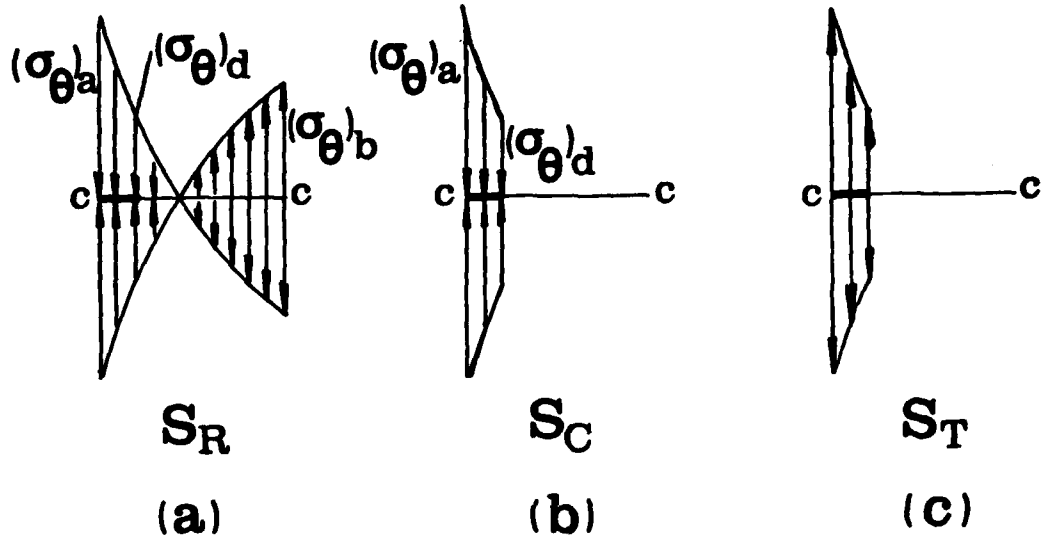

Figure 2(a). Residual stress normal to the cross section cc of a 100% overstrained tube.

Figures 2(b) and (c). Normal transactions on the crack surface.

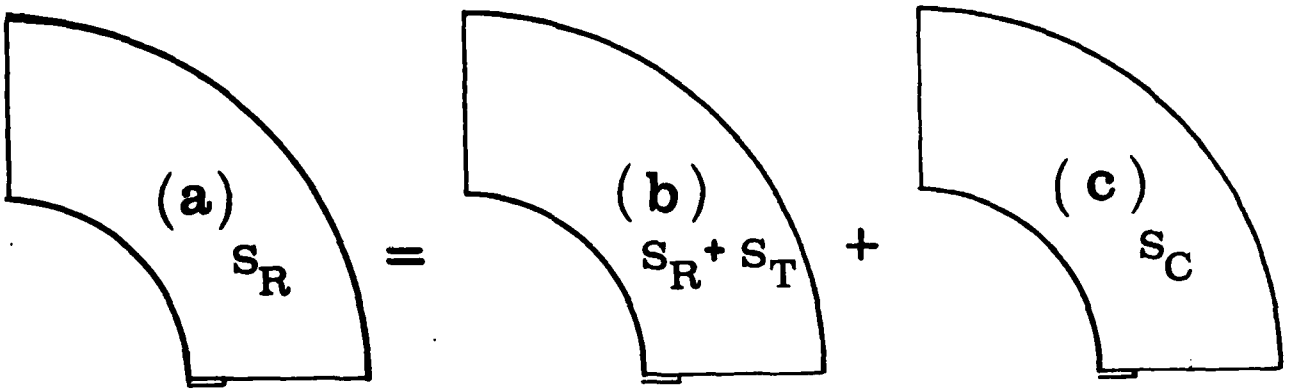

K_1 due to $S_R + S_C + S_T$ = K_1 due to $S_R + S_T$ + K_1 due to S_C

$(K_1)_{S_R}$ = 0 + $(K_1)_{S_C}$

Figure 3. Stress intensity factor due to the residual stress by superposition.

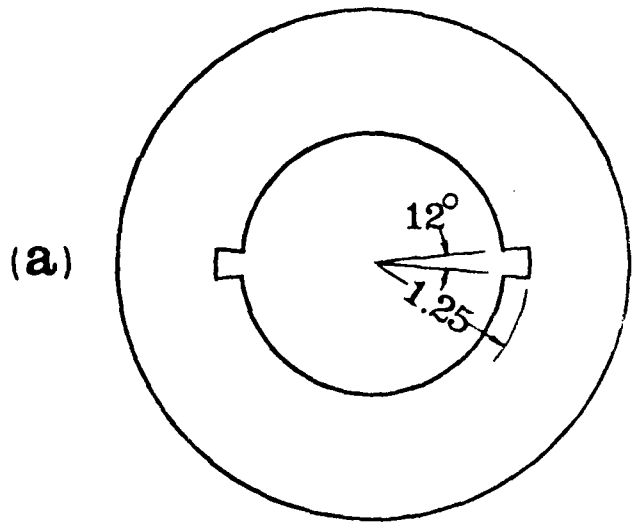

Figure 4(a). Two equal and symmetric notches in a t[illegible].

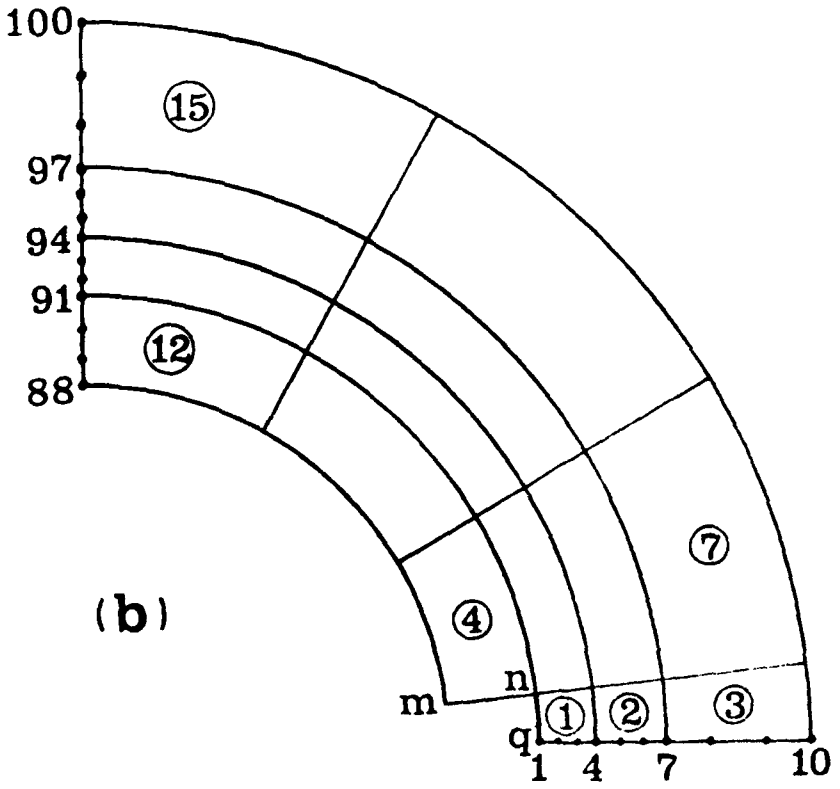

Figure 4(b). Finite element idealization for Figure 4(a).

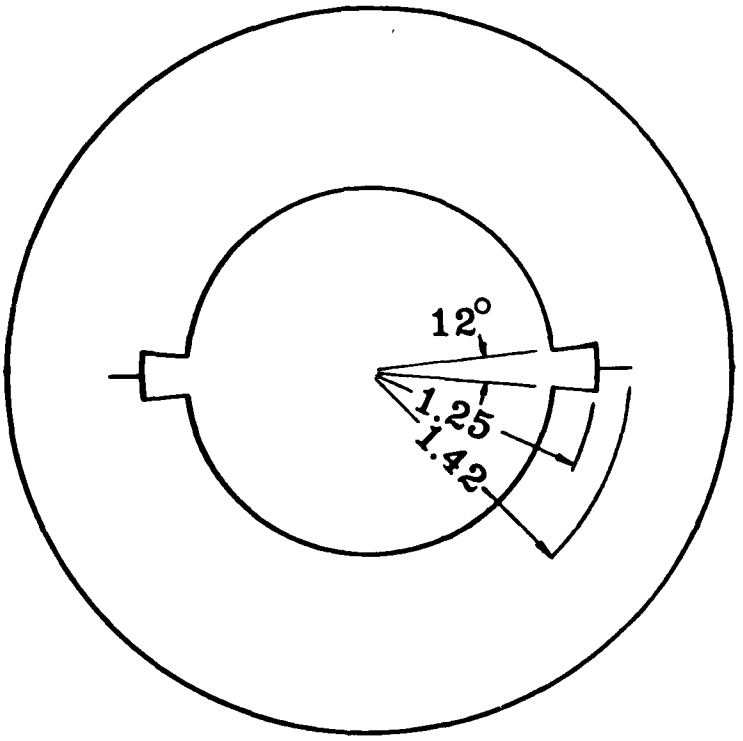

Figure 5. Two equal and symmetric radial cracks initiated from notches in a tube shown previously.

TECHNICAL REPORT EXTERNAL DISTRIBUTION LIST

	NO. OF COPIES
ASST SEC OF THE ARMY RESEARCH & DEVELOPMENT ATTN: DEP FOR SCI & TECH THE PENTAGON WASHINGTON, D.C. 20315	1
COMMANDER US ARMY MAT DEV & READ. COMD ATTN: DRCDE 5001 EISENHOWER AVE ALEXANDRIA, VA 22333	1
COMMANDER US ARMY ARRADCOM ATTN: DRDAR-LC -ICA (PLASTICS TECH EVAL CEN) -LCE -LCM -LCS -LCW -TSS(STINFO) DOVER, NJ 07801	1 1 1 1 1 1 2
COMMANDER US ARMY ARRCOM ATTN: DRSAR-LEP-L ROCK ISLAND ARSENAL ROCK ISLAND, IL 61299	1
DIRECTOR US Army Ballistic Research Laboratory ATTN: DRDAR-TSB-S (STINFO) ABERDEEN PROVING GROUND, MD 21005	1
COMMANDER US ARMY ELECTRONICS COMD ATTN: TECH LIB FT MONMOUTH, NJ 07703	1
COMMANDER US ARMY MOBILITY EQUIP R&D COMD ATTN: TECH LIB FT BELVOIR, VA 22060	1
COMMANDER US ARMY TANK-AUTMV R&D COMD ATTN: TECH LIB - DRDTA-UL MAT LAB - DRDTA-RK WARREN MICHIGAN 48090	1 1
COMMANDER US MILITARY ACADEMY ATTN: CHMN, MECH ENGR DEPT WEST POINT, NY 10996	1
COMMANDER REDSTONE ARSENAL ATTN: DRSMI-RB -RRS -RSM ALABAMA 35809	2 1 1
COMMANDER ROCK ISLAND ARSENAL ATTN: SARRI-ENM (MAT SCI DIV) ROCK ISLAND, IL 61202	1
COMMANDER HQ, US ARMY AVN SCH ATTN: OFC OF THE LIBRARIAN FT RUCKER, ALABAMA 36362	1
COMMANDER US ARMY FGN SCIENCE & TECH CEN ATTN: DRXST-SD 220 7TH STREET, N.E. CHARLOTTESVILLE, VA 22901	1
COMMANDER US ARMY MATERIALS & MECHANICS RESEARCH CENTER ATTN: TECH LIB - DRXMR-PL WATERTOWN, MASS 02172	2

NOTE: PLEASE NOTIFY COMMANDER, ARRADCOM, ATTN: BENET WEAPONS LABORATORY, DRDAR-LCB-TL, WATERVLIET ARSENAL, WATERVLIET, N.Y. 12189, OF ANY REQUIRED CHANGES.

TECHNICAL REPORT EXTERNAL DISTRIBUTION LIST (CONT)

	NO. OF COPIES
COMMANDER US ARMY RESEARCH OFFICE P.O. BOX 12211 RESEARCH TRIANGLE PARK, NC 27709	1
COMMANDER US ARMY HARRY DIAMOND LAB ATTN: TECH LIB 2800 POWDER MILL ROAD ADELPHIA, MD 20783	1
DIRECTOR US ARMY INDUSTRIAL BASE ENG ACT ATTN: DRXPE-MT ROCK ISLAND, IL 61201	1
CHIEF, MATERIALS BRANCH US ARMY R&S GROUP, EUR BOX 65, FPO N.Y. 09510	1
COMMANDER NAVAL SURFACE WEAPONS CEN ATTN: CHIEF, MAT SCIENCE DIV DAHLGREN, VA 22448	1
DIRECTOR US NAVAL RESEARCH LAB ATTN: DIR, MECH DIV CODE 26-27 (DOC LIB) WASHINGTON, D. C. 20375	1 1
NASA SCIENTIFIC & TECH INFO FAC. P. O. BOX 8757, ATTN: ACQ BR BALTIMORE/WASHINGTON INTL AIRPORT MARYLAND 21240	1

	NO. OF COPIES
COMMANDER DEFENSE TECHNICAL INFO CENTER ATTN: DTIA-TCA CAMERON STATION ALEXANDRIA, VA 22314	12
METALS & CERAMICS INFO CEN BATTELLE COLUMBUS LAB 505 KING AVE COLUMBUS, OHIO 43201	1
MECHANICAL PROPERTIES DATA CTR BATTELLE COLUMBUS LAB 505 KING AVE COLUMBUS, OHIO 43201	1
MATERIEL SYSTEMS ANALYSIS ACTV ATTN: DRXSY-MP ABERDEEN PROVING GROUND MARYLAND 21005	1

NOTE: PLEASE NOTIFY COMMANDER, ARRADCOM, ATTN: BENET WEAPONS LABORATORY, DRDAR-LCB-TL, WATERVLIET ARSENAL, WATERVLIET, N.Y. 12189, OF ANY REQUIRED CHANGES.

TECHNICAL REPORT INTERNAL DISTRIBUTION LIST

	NO. OF COPIES
COMMANDER	1
CHIEF, DEVELOPMENT ENGINEERING BRANCH	1
ATTN: DRDAR-LCB-DA	1
-DM	1
-DP	1
-DR	1
-DS	1
-DC	1
CHIEF, ENGINEERING SUPPORT BRANCH	1
ATTN: DRDAR-LCB-SE	1
-SA	1
CHIEF, RESEARCH BRANCH	2
ATTN: DRDAR-LCB-RA	1
-RC	1
-RM	1
-RP	1
CHIEF, LWC MORTAR SYS. OFC. ATTN: DRDAR-LCB-M	1
CHIEF, IMP. 81MM MORTAR OFC. ATTN: DRDAR-LCB-I	1
TECHNICAL LIBRARY ATTN: DRDAR-LCB-TL	5
TECHNICAL PUBLICATIONS & EDITING UNIT ATTN: DRDAR-LCB-TL	2
DIRECTOR, OPERATIONS DIRECTORATE	1
DIRECTOR, PROCUREMENT DIRECTORATE	1
DIRECTOR, PRODUCT ASSURANCE DIRECTORATE	1

NOTE: PLEASE NOTIFY ASSOC. DIRECTOR, BENET WEAPONS LABORATORY, ATTN: DRDAR-LCB-TL, OF ANY REQUIRED CHANGES.


DAT
FILM
4